# Metabolic Imaging of Ovarian Tumors with Carbon-11-Methionine: A PET Study

Maria Lapela, Sirkku Leskinen-Kallio, Matti Varpula, Seija Grénman, Tuula Salmi, Kalle Alanen, Kjell Någren, Pertti Lehikoinen, Ulla Ruotsalainen, Mika Teräs and Heikki Joensuu

*Departments of Oncology and Radiotherapy and Pathology and Turku Medical Cyclotron PET Center, Turku University; and Medical Imaging Center and Department of Obstetrics and Gynecology, Turku University Central Hospital, Turku, Finland*

This study examines the potential of $^{11}$C-methionine as a PET tracer in metabolic imaging of benign and malignant ovarian tumors. **Methods:** Four patients with one or two benign ovarian tumors (endometriomas or cystadenomas), two patients with a tumor of borderline malignancy and seven patients with ovarian cancer were studied with $^{11}$C-methionine and PET before laparotomy. CT or MRI were performed as a reference. Tracer uptake was quantitated by calculating tracer standardized uptake values (SUVs) and the kinetic influx constants ($K_i$ values). **Results:** Benign or borderline malignant tumors did not accumulate $^{11}$C-methionine, whereas all carcinomas had significant uptake. The mean SUV of the primary carcinomas was 7.0 (s.d., 2.2), and the mean $K_i$ was 0.14 $min^{-1}$ (s.d., 0.1 $min^{-1}$), but the distribution of tracer uptake was highly heterogenous in four of six tumors. **Conclusion:** Ovarian cancer can be imaged with $^{11}$C-methionine and PET. This method also may be of value in the differential diagnosis between benign and malignant ovarian neoplasms. Due to physiological accumulations and methodological limitations, the value of $^{11}$C-methionine PET in the staging of ovarian cancer appears to be limited.

**Key Words:** positron emission tomography; carbon-11-methionine; ovarian cancer

**J Nucl Med 1995; 36:2196–2200**

Ovarian cancer is the most lethal of all gynecologic cancers. At its early stages, symptoms are rarely present, and therefore in about two-thirds of cases the disease has already spread beyond the pelvis at the time of diagnosis (*1*). Stage at diagnosis is one of the major prognostic factors in ovarian cancer (*2*). The diagnosis and staging of ovarian cancer are currently based on surgery and histopathological findings, although modern imaging techniques have been introduced for preoperative evaluation of the disease (*3*). Ultrasonography, CT and MRI, however, lack the potential for distinguishing benign reactive changes from cancer infiltration (*4*).

Metabolic imaging with PET has been shown to be an effective method to detect cancer. The first PET studies on ovarian cancer were done with [$^{18}$F]fluoro-2-deoxy-D-glucose ([$^{18}$F]FDG). Wahl et al. demonstrated accumulation of [$^{18}$F]FDG into ovarian adenocarcinoma in a nude mouse model (*5*) and later found it feasible to image human ovarian cancer with [$^{18}$F]FDG and PET (*6*). It has been suggested that PET with [$^{18}$F]FDG may have potential in the differential diagnosis between malignant and benign ovarian tumors (*7*) and in imaging recurrent ovarian carcinoma (*8,9*), but results have not been consistent (*10*).

An essential amino acid, methionine, labeled with $^{11}$C (L-[methyl-$^{11}$C]methionine, $^{11}$C-methionine), has been found to be a valuable tracer for metabolic imaging of human cancer. Brain (*11*) and lung tumors (*12*), non-Hodgkin's lymphoma (*13*), breast cancer (*14*), head and neck cancer (*15*) and uterine carcinoma (*16*) have already been successfully studied with $^{11}$C-methionine and PET. Furthermore, high uptake of $^{11}$C-methionine may correlate with poor histological grade of differentiation in brain (*17*), lung (*18*) and uterine (*16*) cancer and with high cell proliferation rates in carcinomas of the breast (*14*) and lung (*19*), which suggests that tissue uptake of methionine may reflect the biological aggressiveness of cancer.

In this study, we investigated the potential of $^{11}$C-methionine as a tracer for PET in imaging of human ovarian tumors.

## METHODS

### Patients

Thirteen patients (aged 26–69 yr, mean 54 yr) with ovarian neoplasms admitted to the Department of Obstetrics and Gynecology at Turku University Central Hospital between March 1993 and March 1994 participated in the study. Twelve patients had a primary ovarian tumor and one patient had a recurrent tumor. The body mass index (BMI) calculated as weight in kilograms divided by the square of height in meters (*20*) varied from 19.9 to 41.7 kg/m$^2$ (median, 25.3 kg/m$^2$).

All patients underwent surgery within 1 mo after the PET study. Based on histopathology of the specimens taken at surgery, seven women had ovarian carcinoma, two had an ovarian tumor of borderline malignancy and four had one or two benign neoplasms of the ovary (either endometriomas or serous or mucinous cystadenomas, Table 1). The seven malignant tumors consisted of four adenocarcinomas of endometrioid type (one of which was a recurrent cancer), two serous cystadenocarcinomas and one clear-cell carcinoma. One of the two tumors of borderline malignancy was

Received Aug. 25, 1994; revision accepted Jan. 16, 1995.

For correspondence or reprints contact: Maria Lapela, MD, Department of Oncology and Radiotherapy, Turku University Central Hospital, FIN-20 520 Turku, Finland.

**TABLE 1**
Tumor Characteristics and Imaging Results

| Patient no. | Histology, grade and FIGO stage | Tumor size (cm) | Size of solid component (cm) | Cyst wall thickness (mm) | CA 12-5 (IU/liter) | SUV | $K_i$ ($min^{-1}$) |
|---|---|---|---|---|---|---|---|
| 1 | Serous cystadenoma | 4 × 3 × 5 | no | 10 | 53 | 1.3 | 0.03 |
| | Endometrioma | 4 × 3 × 5 | no | 15 | | 1.8 | 0.04 |
| 2 | Endometrioma | 6 × 5 × 9 | no | <3 | n.d. | 1.9 | 0.03 |
| 3 | Endometrioma | 8 × 9 × 12 | no | <3 | 230 | 2.3 | 0.04 |
| | Endometrioma | 4 × 4 × 5 | no | <3 | | 2.7 | 0.05 |
| 4 | Mucinous cystadenoma | 7 × 6 × 4 | 3 × 2 × 2 | n.d. | n.d. | 3.6 | 0.05 |
| 5 | Mucinous cystadenoma | 14 × 20 × 19 | 12 × 1 × 2 | n.d. | 43 | 2.6 | 0.04 |
| 6 | Mixed neoplasm | 8 × 7 × 7 | no | <3 | 63 | 2.3 | 0.05 |
| 7 | Serous, Grade 1, Stage IIIC | 9 × 7 × 8 | 5 × 2 × 2 | n.d. | 1680 | 3.9 | 0.05 |
| | | 5 × 6 × 6 | 3 × 1 × 3 | n.d. | | | |
| | | 3 × 3 × 4 | 2 × 2 × 2 | n.d. | | | |
| | | 3 × 3 × 3 | no | <3 | | | |
| | | 3 × 3 × 4 | 2 × 2 × 2 | n.d. | | | |
| 8 | Serous, Grade 2, Stage IIIC | n.m. | | | 3300 | 7.5 | 0.09 |
| 9 | Endometrioid, Grade 2, Stage IA | 7 × 12 × 7 | 2 × 7 × 7 | n.d. | 195 | 8.4 | 0.17 |
| | | | 3 × 3 × 3 | n.d. | | | |
| 10 | Clear-cell, Grade 2, Stage IIB | 13 × 20 × 19 | 12 × 5 × 9 | n.d. | 308 | 10.2 | 0.32 |
| 11 | Endometrioid, Grade 3, Stage IV | 17 × 15 × 18 | no | <3 | 2040 | 5.3 | 0.08 |
| | | 5 × 10 × 6 | 5 × 10 × 6 | no | | | |
| 12 | Endometrioid, Grade 3, Stage IV | n.m. | | | 660 | 6.5 | 0.15 |
| 13 | Endometrioid, Grade 3, recurrent ca. | 6 × 5 × 8 | 6 × 5 × 8 | no | 86 | 8.0 | 0.14 |

n.d. = not determined; n.m. = not measurable; ca. = carcinoma.

mucinous cystadenoma and the other a neoplasm of mixed type that consisted of a borderline malignant Brenner's tumor and serous cystadenoma. Histological investigation and grading were done without knowledge of the PET data. Surgical staging of the cancers was done according to the International Federation of Gynecology and Obstetrics (FIGO) (*21*).

All PET studies of the primary neoplasms were performed prior to any treatment for ovarian tumors. Patient 8 had been irradiated for cervical cancer 27 yr earlier. In Patient 13, the recurrence occured 5 yr after the primary surgery and following chemotherapy. All patients had fasted for at least 4 hr before imaging.

Written informed consent was obtained from all patients. The study was approved by the Ethical Committee of Turku University Central Hospital.

### Morphologic Imaging

CT was performed before surgery for morphologic reference imaging and accurate localization of the sites of interest in all but one of patient. The slice thickness was 5 or 10 mm. Intravenous contrast enhancement was used in every patient except Patient 12, who was allergic to the iodine-containing contrast agent. Patient 6 was imaged with MRI. T2-weighted axial and sagittal images were obtained, with a slice thickness of 10 mm. PET and CT/MR imaging were performed within 7 days except in Patient 4, for whom the time interval was 18 days. The scans were interpreted by one radiologist with expertise in radiology of the female genital organs without knowledge of the results of the PET study or surgical and histological findings.

### PET

Carbon-11-methionine was synthesized at the Radiopharmaceutical Chemistry Laboratory of Turku University Cyclotron/PET Center as described by Långström et al. (*22*) with slight modifications. The radiochemical purity of the tracer was measured as described elsewhere (*23*) and was over 94% (median, 96.8%). The impurities were $^{11}$C-methionine sulfoxide and D-[$^{11}$C]methionine, which were present in about equal amounts.

The PET scanner used in the study acquires 15 contiguous slices simultaneously with an axial resolution of 6.7 mm and spatial resolution of 6.5 mm measured according to Spinks et al. (*24*).

To correct for photon attenuation, a transmission scan was obtained prior to emission imaging with a removable ring source containing $^{68}$Ge (total collected counts over 150 × $10^6$). A bolus of $^{11}$C-methionine (mean 303 MBq; range 280–350 MBq) was injected into a peripheral vein of the upper extremity and dynamic emission acquisition followed for 40 min (4 × 30 sec, 3 × 60 sec, 5 × 180 sec and 4 × 300 sec). All data were corrected for deadtime, decay and photon attenuation and were reconstructed in a 256 × 256 matrix with a Hann filter (cutoff frequency 0.5).

Radioactivity in plasma was measured from 16 to 21 blood samples taken from an antecubital vein of the preheated arm contralateral to the injection site. The low molecular weight fraction of plasma taken at 20–25, 40, and 60 min after injection was separated by fast-gel filtration for radioactivity measurements (*25*).

### Image Analysis

Dynamic frames were summed together from 5 to 40 min, and localization in the tissues of interest was confirmed using the CT or MR images. Comparison was made visually by comparing the PET images printed on paper with CT/MR images on film. Regions of interest (ROIs) were drawn on the hot spots of both the tumors and normal tissues in the last frame of the dynamic image. ROIs in the normal tissues were drawn in the acetabulum, iliac and sacral bones, bladder and the intestinal area, if they were clearly visible and reliably identifiable on the last dynamic image. ROIs

with the maximum average counts were selected to represent $^{11}$C-methionine uptake in the tissues.

Tracer accumulation in the ROIs was measured using the standardized uptake value (SUV), which is the activity concentration in a ROI divided by the injected dose normalized to the patient's weight (*26*). The $^{11}$C-methionine uptake rate from the plasma into the tissue was calculated as influx constants ($K_i$ values) using the Patlak et al. (*27*) graphical method, an approach in which the input function was originally based on arterial samples. The activity concentration of the low molecular weight fraction of plasma was used as the input function. The last eight data points representing the time from 8 to 40 min after the tracer injection were used to produce the influx curve.

### Statistical Analysis

The quantitative results between different groups were compared with Student's t-test for unpaired data. All p values are two-sided.

## RESULTS

### Benign and Borderline Malignant Tumors

There was little uptake of $^{11}$C-methionine in histologically proven benign tumors or the two tumors of borderline malignancy. In two patients with ovarian endometriomas (Patients 2 and 3), the tumors were seen in the PET image as areas with little tracer uptake (Fig. 1), while one endometrioma, a serous cystadenoma (Patient 1) and a mucinous cystadenoma (Patient 4) were not clearly distinguishable from the adjacent tissues in the PET scan. Similarly, a mucinous cystadenoma of borderline malignancy (Patient 5) and a borderline neoplasm with composite histology (Patient 6) presented as a cold area with less activity than was found in the surrounding normal tissues (Fig. 2). The mean SUV of the benign tumors was 2.3 (s.d. 0.7; range 1.3–3.6) and the mean $K_i$ 0.04 min$^{-1}$ (s.d. 0.01 min$^{-1}$; range 0.03–0.05 min$^{-1}$).

### Primary Carcinomas

Unlike the benign and borderline malignant tumors, all primary carcinomas accumulated $^{11}$C-methionine, but the distribution of uptake within the tumors was usually heterogenous. Four of the six primary carcinomas had both cystic and solid components. In these patients, the cysts appeared as black areas with no clear uptake of $^{11}$C-methionine, while the solid parts of the tumors were visible (Fig. 3). Precise delineation of the carcinomas from the adjacent tissues was often difficult in the PET image. The mean SUV of the hot spot regions of the six primary carcinomas was 7.0 (s.d. 2.2; range 3.9–10.2), and the mean $K_i$ was 0.1 min$^{-1}$ (s.d. 0.1 min$^{-1}$; range 0.05–0.33 min$^{-1}$). The difference between the SUVs and the $K_i$ values of malignant and benign tumors was significant ($p < 0.001$ for SUVs, $p = 0.007$ for $K_i$). There did not appear to be any correlation between the SUVs and $K_i$ values of the malignant tumors and histological grade, FIGO stage or serum CA 12-5 levels, although the smallest SUV and $K_i$ were measured in our only patient with well-differentiated carcinoma (Table 1). In addition to the ovarian tumor with a SUV of 7.5, two inguinal 3-cm lymph node metastases with SUVs of 6.3 and 5.5 were visualized in Patient 8.

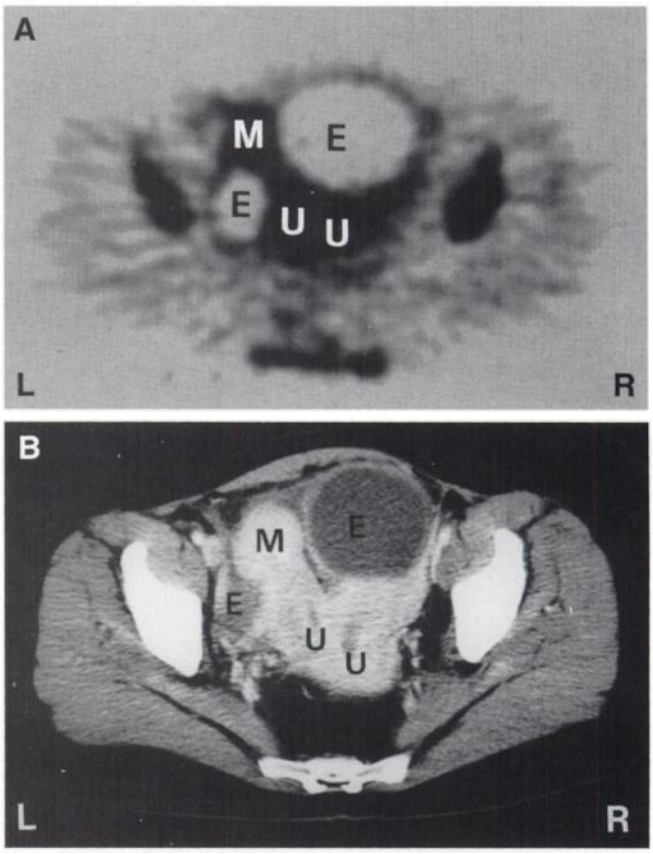


**FIGURE 1.** (A) PET and (B): CT images of Patient 3 with a duplex uterus (U). There are two large endometriomas (E), one in each ovary, with no accumulation of methionine, and one leiomyoma in the left uterus (M) with a SUV of 3.5. The hip joints and the sacrum also accumulated $^{11}$C-methionine.

The recurrent ovarian cancer (Patient 13) turned out to be a solid tumor without cystic regions at surgery. The tumor was clearly visualized on the PET study as a homogenous hot spot with a SUV of 8.0 and a $K_i$ of 0.14 min$^{-1}$ (Table 1).

### Physiological Accumulations of Carbon-11-Methionine in the Lower Abdomen

The bowel clearly accumulated $^{11}$C-methionine. The mean SUV of the bowel in patients with no peritoneal carcinosis at surgery was 5.7 (n = 5; s.d. 1.8) (Fig. 4) and 5.9 in the two patients (Patients 7 and 12) with peritoneal carcinosis.

Physiological accumulation of $^{11}$C-methionine also was detected in the endometrium and pelvic bones. The mean SUV of the benign endometrium was 4.7 (n = 4, s.d. 0.9), the acetabulum 4.8 (n = 8; s.d. 1.1), iliac bone 5.1 (n = 7; s.d., 1.4) and sacral bone 5.3 (n = 7; s.d. 1.4, Fig. 4). The mean $K_i$ value of the benign endometrium was 0.10 min$^{-1}$ (n = 4, s.d. 0.04 min$^{-1}$), acetabulum 0.09 min$^{-1}$ (n = 8; s.d. 0.02 min$^{-1}$), iliac bone 0.09 min$^{-1}$ (n = 7; s.d. 0.01 min$^{-1}$), and sacral bone 0.10 min$^{-1}$ (n = 7; s.d. 0.02 min$^{-1}$). The

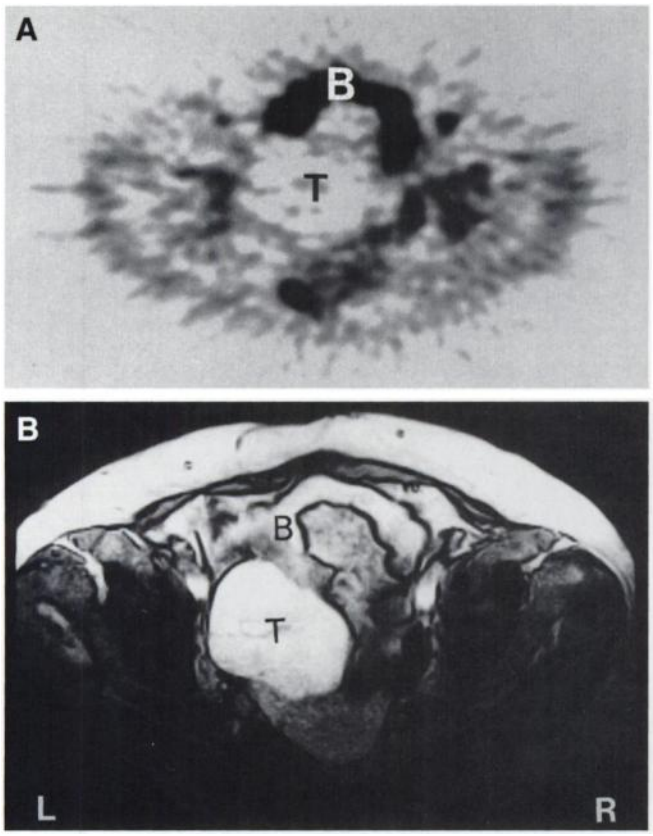


**FIGURE 2.** (A) PET and (B) MR images of Patient 6 with mixed neoplasm (T) of the ovary with no accumulation of methionine. High accumulation is seen in the bowel, especially on the ventral side of the tumor (B).

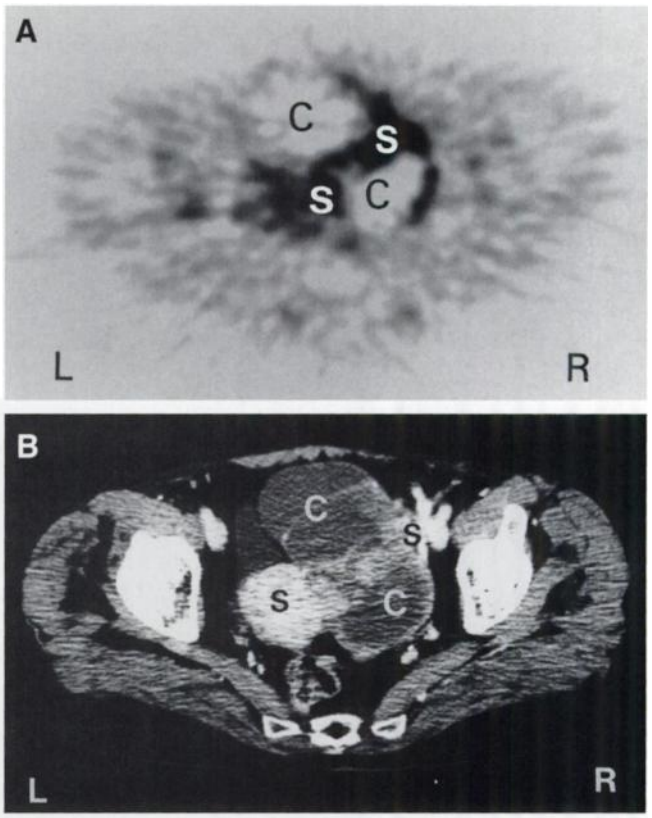


**FIGURE 3.** (A) PET and (B) CT images of Patient 9 with endometrioma. The tumor was large and cystic (C) with solid components (S) where the SUV and the $K_i$ value were measured.

bladder was visualized in Patients 6 and 8, with SUVs of 7.9 and 11.7, respectively.

The SUVs of $^{11}$C-methionine in ovarian cancer were higher than those in the acetabulum ($p = 0.02$) or the iliac bone ($p = 0.05$) and tended to be higher than those in the endometrium ($p = 0.06$) or sacral bone ($p = 0.08$), but no such difference was found between $^{11}$C-methionine uptake in cancer and the bowel ($p = 0.27$). No such associations were found when the $K_i$ values measured in ovarian cancer and those found in the normal tissues were compared ($p > 0.1$ for all comparisons).

## DISCUSSION

In the present series, all malignant ovarian tumors significantly accumulated $^{11}$C-methionine, whereas benign or borderline malignant neoplasms did not. These results suggest that PET with $^{11}$C-methionine might help in distinguishing benign from malignant ovarian tumors. Only one of the primary cancers in this series, however, manifested as a homogenous hot spot (Patient 9); the remaining carcinomas had irregular patterns of tracer uptake. This is in accordance with the pathology of most ovarian carcinomas, since these neoplasms are often partly cystic and the soft-tissue component may be scanty. In many subtypes of benign tumors, the solid components may be even smaller, and the cyst walls can be only a few millimeters thick. Thus, tracer accumulation in only a few millimeter thick layers of tissue may not be detected with the resolution capacity of current PET equipment. The partial volume effect may also diminish the potential for their detection.

Physiological uptake of $^{11}$C-methionine in normal tissues can be used as a landmark when locating lesions in a PET

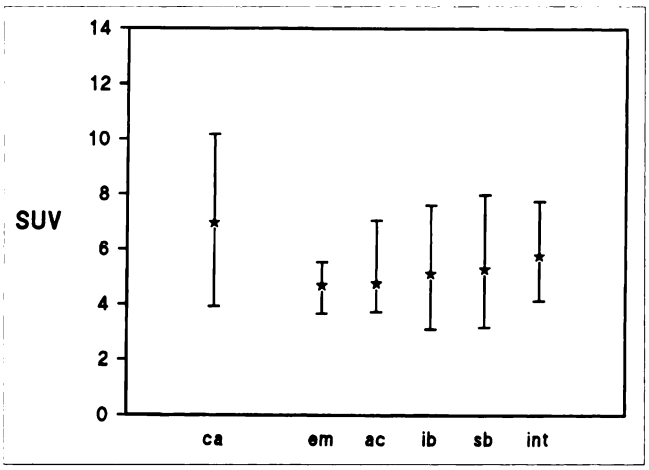


**FIGURE 4.** SUVs of malignant and some normal tissues (mean and range). ca = primary ovarian cancer (n = 6); em = benign endometrium (n = 4); ac = the acetabulum (n = 8); ib = the iliac bone (n = 7); sb = the sacral bone (n = 7); int = normal intestinal area (n = 5).

study (e.g., in the head and neck region). In the lower abdominal area, variable and quite high accumulation of $^{11}$C-methionine in the bowel interferes markedly with the localization and delineation of tumors, even if CT or MRI are used as a reference. Hence, staging of ovarian cancer is hampered by active physiological uptake in the intestine, and malignant lymph nodes with small cancer deposits and peritoneal implants of cancer may be masked by $^{11}$C-methionine uptake in the bowel.

Ovarian cancer has been reported to be successfully imaged with [$^{18}$F]FDG PET (*6–10*). Fluorine-18-FDG may have some advantages if compared to $^{11}$C-methionine for imaging lesions located in the lower abdomen. FDG is excreted into the urine, and high amounts of the tracer are seen in the kidneys and bladder. These organs are usually easy to identify in a PET image, and the bladder can be irrigated during the scan. It is, however, currently unresolved if [$^{18}$F]FDG is effective in detecting small intra-abdominal metastases of ovarian cancer (*10*). Furthermore, most of the [$^{18}$F]FDG PET studies reported have consisted of recurrent ovarian tumors (*8–10*) and only a few patients with primary ovarian cancer have been imaged with [$^{18}$F]FDG.

Uptake of $^{11}$C-methionine measured in the benign endometrium was similar to values from our earlier study and it was lower than that in endometrial cancer (*16*). Although nine patients had the bladder in the field of view, only two of them had clear accumulation of activity in the bladder. They had no known disease of the kidneys or the bladder, serum creatinine levels were normal as were urine sediment analyses. Bladder irrigation was not used in this study. We have observed similar variability in bladder activity in an earlier study (*16*).

## CONCLUSION

All seven histologically confirmed malignant ovarian tumors, unlike the benign or the borderline malignant tumors, accumulated $^{11}$C-methionine. The often cystic structure of ovarian neoplasms however, and the relatively high physiological accumulations of $^{11}$C-methionine in the bowel may hamper tumor detection and therefore small tumor deposits such as lymph node metastases and peritoneal implants of cancer are difficult to detect with $^{11}$C-methionine. Therefore, further studies are needed to establish the value of $^{11}$C-methionine and PET in the differential diagnosis between benign and malignant ovarian tumors using strict coregistration and fusion of CT/MR and PET images. The usefulness of $^{11}$C-methionine PET in detecting recurrent ovarian cancer also requires study.

## ACKNOWLEDGMENTS

The authors thank Professors Eeva Nordman and Uno Wegelius for their valuable support, the personnel of the Cyclotron/PET Center, Imaging Center and Department of Obstetrics and Gynecology for their cooperation. This study was financially supported by the Finnish Cancer Society and the Turku University Foundation.

## REFERENCES

1. Cannistra SA. Cancer of the ovary. *N Engl J Med* 1993;329:1550–1559.
2. Omura GA, Brady MF, Homesley HD, et al. Long-term follow-up and prognostic factor analysis in advanced ovarian carcinoma: the Gynecologic Oncology Group experience. *J Clin Oncol* 1991;9:1138–1150.
3. Hricak H. Carcinoma of the female reproductive organs. Value of cross-sectional imaging. *Cancer* 1991;67:1209–1218.
4. Bragg DG, Hricak H. Imaging in gynecologic malignancies. *Cancer* 1993;71: 1648–1651.
5. Wahl RL, Hutchins GD, Buchsbaum DJ, Liebert M, Grossman HB, Fisher S. Fluorine-18-2-deoxy-2-fluoro-D-glucose uptake into human tumor xenografts. *Cancer* 1991;67:1544–1550.
6. Wahl RL, Hutchins G, Roberts J. FDG-PET imaging of ovarian cancer: initial evaluation in patients. [Abstract]. *J Nucl Med* 1991;32(suppl):982P.
7. Hubner KF, McDonald TW, Niethammer JG, Smith GT, Gould HR, Buonocore E. Assessment of primary and metastatic ovarian cancer by positron emission tomography (PET) using 2-[$^{18}$F]deoxyglucose. *Gynecol Oncol* 1993;51:197–204.
8. Karlan BY, Hawkins R, Hoh C, et al. Whole-body positron emission tomography with 2-[$^{18}$F]-fluoro-2-deoxy-D-glucose can detect recurrent ovarian carcinoma. *Gynecol Oncol* 1993;51:175–181.
9. Casey MJ, Gupta NC, Muths CK. Experience with positron emission tomography (PET) scans in patients with ovarian cancer. *Gynecol Oncol* 1994;53: 331–338.
10. Holdeman KP, McIntosh DG, Smith ML, et al. PET imaging of ovarian cancer prior to second look laparotomy [Abstract]. *J Nucl Med* 1994; 35(suppl):117P.
11. Ericson K, Lilja A, Bergström M, et al. Positron emission tomography with ([$^{11}$C]methyl)-L-methionine, [$^{11}$C]-D-glucose, and [$^{68}$Ga]EDTA in supratentorial tumors. *J Comput Assist Tomogr* 1985;9:683–689.
12. Kubota K, Matsukawa T, Ito M, et al. Lung tumor imaging by positron emission tomography using carbon-11-L-methionine. *J Nucl Med* 1985;26:37–42.
13. Leskinen-Kallio S, Ruotsalainen U, Någren K, Teräs M, Joensuu H. Uptake of carbon-11-methionine and fluorodeoxyglucose in non-Hodgkin's lymphoma: a PET study. *J Nucl Med* 1991;32:1211–1218.
14. Leskinen-Kallio S, Någren K, Lehikoinen P, Ruotsalainen U, Joensuu H. Uptake of [$^{11}$C]methionine in breast cancer studied by PET. *Br J Cancer* 1991;64:1121–1124.
15. Leskinen-Kallio S, Någren K, Lehikoinen P, Ruotsalainen U, Teräs M, Joensuu H. Carbon-11-methionine and PET is an effective method to image head and neck cancer. *J Nucl Med* 1992;33:691–695.
16. Lapela M, Leskinen-Kallio S, Varpula M, et al. Imaging of uterine carcinoma by carbon-11-methionine and PET. *J Nucl Med* 1994;35:1618–1623.
17. Derlon JM, Bourdet C, Bustany P, et al. Carbon-11-methionine uptake in gliomas. *Neurosurgery* 1989;25:720–728.
18. Fujiwara T, Matsukawa T, Kubota K, et al. Relationship between histologic type of primary lung cancer and carbon-11-L-methionine uptake with positron emission tomography. *J Nucl Med* 1989;30:33–37.
19. Miyazawa H, Arai T, Iio M, Hara T. PET imaging of non-small-cell lung carcinoma with carbon-11-methionine: relationship between radioactivity uptake and flow-cytometric parameters. *J Nucl Med* 1993;34:1886–1891.
20. Olefsky JM. Obesity. In: Wilson JD, Braunwald E, Isselbacher KJ, et al. eds. *Harrisons's principles of internal medicine*, volume 1, 12th ed. New York: McGraw-Hill; 1991:411.
21. Revised FIGO staging for gynaecological cancer. *Br J Obstet Gynecol* 1989; 96:889–892.
22. Långström B, Antoni G, Gullberg P, et al. Synthesis of L- and D-[methyl-$^{11}$C]methionine. *J Nucl Med* 1987;28:1037–1040.
23. Någren K. Quality control aspects in the preparation of [$^{11}$C]methionine. In: Mazoyer BM, Heiss WD, Comar D, eds. *PET studies on amino acid metabolism and protein synthesis*. Dordrecht: Kluwer; 1993:81–87.
24. Spinks TJ, Jones T, Gilardi MC, Heather JD. Physical performance of the latest generation of commercial positron scanners. *IEEE Trans Nucl Sci* 1988;35:721–725.
25. Lundqvist H, Stålnacke C-G, Långström B, Jones B. Labeled metabolites in plasma after i.v. administration of [$^{11}CH_3$]-L-methionine. In: Greits T, Widen L, Ingvar D, eds. *The metabolism of the human brain studies with positron emission tomography*. New York: Raven Press; 1985:233–240.
26. Woodard HW, Bigler RB, Freed B, Russ G. Expression of tissue isotope distribution. *J Nucl Med* 1975;16:958–959.
27. Patlak CS, Blasberg RG, Fenstermacher JD. Graphical evaluation of blood-to-brain transfer constants from multiple-time uptake data. *J Cereb Blood Flow Metab* 1983;3:1–7.